Infrared Studies of the CO-Inhibited Form of the Fe-Only Hydrogenase from Clostridium pasteurianum I: Examination of Its Light Sensitivity at Cryogenic Temperatures †

6 AUTHORS, INCLUDING:

Kimberly A Bagley
State University of New York College at Buffalo

30 PUBLICATIONS   **2,131** CITATIONS

Infrared Studies of the CO-Inhibited Form of the Fe-Only Hydrogenase from *Clostridium pasteurianum* I: Examination of Its Light Sensitivity at Cryogenic Temperatures[†]

Zhujun Chen,[‡] Brian J. Lemon,[§] Shan Huang,[‡] Derrick J. Swartz,[‡] John W. Peters,[§] and Kimberly A. Bagley*[,‡]

*Department of Chemistry, Buffalo State, State University of New York, Buffalo, New York 14222, and
Department of Chemistry and Biochemistry, Utah State University, Logan, Utah 84322*

ABSTRACT: Infrared spectroscopy has been used to examine the oxidized and CO-inhibited forms of Fe-only hydrogenase I from *Clostridium pasteurianum*. For the oxidized enzyme, five bands are detected in the infrared spectral region between 2100 and 1800 cm^{-1}. The pattern of infrared bands is consistent with the presence of two terminally coordinated carbon monoxide molecules, two terminally coordinated cyanide molecules, and one bridging carbon monoxide molecule, ligated to the Fe atoms of the active site [2Fe] subcluster. Infrared spectra of the carbon monoxide-inhibited state, prepared using both natural abundance CO and ^{13}CO, indicate that the two terminally coordinated CO ligands that are intrinsic to the enzyme are coordinated to different Fe atoms of the active site [2Fe] subcluster. Irradiation of the CO-inhibited state at cryogenic temperatures gives rise to two species with dramatically different infrared spectra. The first species has an infrared spectrum identical to the spectrum of the oxidized enzyme, and can be assigned as arising from the photolysis of the exogenous CO from the active site. This species, which has been observed in X-ray crystallographic measurements [Lemon, B. J., and Peters, J. W. (2000) *J. Am. Chem. Soc. 122*, 3793], decays above 150 K. The second light-induced species decays above 80 K and is characterized by loss of the infrared band associated with the Fe bridging CO at 1809 cm^{-1}. Potential models for the second photolysis event are discussed.

Hydrogenases catalyze the reversible oxidation of molecular hydrogen into protons in a wide variety of microorganisms. Most known hydrogenases can oxidize hydrogen in the absence of additional substrates and contain metal ions at their active sites. These enzymes can be classified into two main groups according to their active site structure. (1) The [NiFe] hydrogenases contain a Ni−Fe dinuclear active site in which the Ni and Fe are bridged via two conserved cysteine thiolates (*1, 2*). The active site is further tethered to the protein via Ni ion coordination to two terminally coordinated cysteine residues. An unusual aspect of the [NiFe] hydrogenase active site is the presence of three diatomic ligands coordinated to the active site Fe. In the case of the [NiFe] hydrogenase from *Allochromatium vinosum*, these ligands have been conclusively demonstrated to be a CO and two CN ligands coordinated to the active site Fe in a terminal fashion (*3−8*). (2) The Fe-only hydrogenases contain an unusual six-Fe cluster in their active site termed the H-cluster. The X-ray crystallographic structures of the Fe-only hydrogenases from both *Clostridium pasteurianum* I (CpI)[1] (*9*) and *Desulfovibrio desulfuricans* (*10*) show that four of the Fe ions are contained in a cubane and that the other two ions form an unusual [2Fe] subcluster as shown
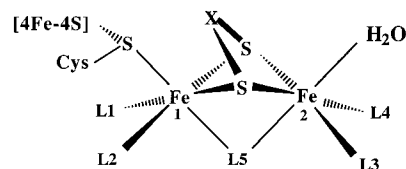

FIGURE 1: Molecular model of the H-cluster from *C. pasteurianum* I, where X represents a covalently linked bridge of unknown composition. L1−L5 have been proposed to arise from CO and CN$^-$ ligands.

in Figure 1. The cubane and [2Fe] subcluster are bridged via a single cysteine thiolate. In the X-ray crystallographic structure of CpI, the two Fe ions of the subcluster are bridged via two sulfur atoms which appear themselves to be bridged by a covalent linkage of multiple light atoms (depicted in Figure 1 as X). The X-ray crystallographic structure of the enzyme from *D. desulfuricans* indicates a similar feature and has been tentatively assigned as either a propanedithiol or a bis(thiomethyl)amine. The crystallographic structures also indicate additional nonprotein ligands coordinated the Fe ions of the [2Fe] subcluster. Infrared spectroscopic studies on the enzymes from *Desulfovibrio vulgaris* and *D. desulfuricans* (*7, 11, 12*) suggest that these ligands may be two CO and two CN ligands that are terminally coordinated to the two active site Fe ions (L1−L4) and that L5 may arise from an

* To whom correspondence should be addressed. E-mail: bagleyka@buffalostate.edu.
[‡] State University of New York.
[§] Utah State University.

[1] Abbreviations: CpI, Fe-only hydrogenase I from *C. pasteurianum*; thionin, 3,7-diamino-5-phenothiazinium; FTIR, Fourier transform infrared.

Fe bridging carbon monoxide ligand. This paper will further address the nature of these ligands in the Fe-only hydrogenase I from *C. pasteurianum* (CpI).

The Fe-only hydrogenases generally function as hydrogen evolution enzymes accepting electrons from a variety of physiological electron carriers and reducing protons into dihydrogen in the process. These hydrogenases are excellent catalysts. Under optimum conditions, the *C. pasteurianum* hydrogenase I can produce 6000 molecules of hydrogen per second at 30 °C.

Three different states of the Fe-only hydrogenases are known which differ in EPR signals associated with the H-cluster. The oxidized form of Fe-only hydrogenases can be prepared either by the anaerobic addition of a redox dye, e.g., thionin, or by allowing the enzyme to become "autoxidized" by evolving H_2 under Ar (*13*). The H-cluster of the oxidized CpI Fe-only hydrogenase exhibits a rhombic EPR signal with *g* values of 2.10, 2.04, and 2.00 arising from an $S = \frac{1}{2}$ system (termed the rhombic 2.10 signal). This signal disappears upon reduction of the enzyme with either dithionite or hydrogen.

A CO-inhibited form of the enzyme formed by exposing the oxidized state to CO was first reported by Erbes et al. (*14*). Lemon and Peters (*15*) have shown that CO binds to CpI in a reversible fashion. Exposure of the oxidized enzyme to CO quantitatively converts the rhombic 2.10 EPR signal into an axial signal, where *g* = 2.074 and 2.011 (termed the axial 2.07 signal). Upon irradiation at cryogenic temperatures, the axial 2.07 signal associated with the CO-inhibited state is replaced by a mixture of two EPR signals (*16*). The relative proportion of the two photoinduced EPR signals is dependent on the temperature at which the irradiation is carried out. Irradiation at 8 K converts the axial 2.07 signal into a rhombic signal with *g* values of 2.10, 2.04, and 2.00. This species is indistinguishable from the rhombic 2.10 signal of the oxidized state. Irradiation at higher temperatures leads to a mixture of two signals consisting of a superposition of the rhombic 2.10 signal and a new rhombic signal at *g* values of 2.26, 2.12, and 1.89 (termed the rhombic 2.26 signal). Increasing the temperature above 200 K leads to the disappearance of both signals and the reappearance of the axial 2.07 signal of the CO-inhibited state. A detailed temperature study shows that the rhombic 2.26 signal reverts to the axial 2.07 signal upon incubation of the sample in the dark above 80 K, while the rhombic 2.10 signal reverts back above 150 K. Photoconversion of the CO-induced axial 2.07 signal into a rhombic 2.10 signal has been hypothesized to arise from the photolysis of the exogenously added CO from the H-cluster. The nature of the second photoinduced intermediate (the rhombic 2.26 signal) is not understood. An additional unexplained feature is that the addition of low concentrations of O_2 to the oxidized enzyme induces an axial 2.07 EPR signal with the same relaxation properties and photolytic properties as the CO-induced signal.

X-ray crystallographic studies on the CO-inhibited form of CpI demonstrate that CO binds to an Fe atom of the [2Fe] subcluster at a site occupied by a terminally bound water molecule in the as-crystallized native state (assumed to be an oxidized state of the enzyme) (*17*). This exogenously added CO can be photochemically cleaved using irradiation from a helium–neon laser at 80–100 K (*18*). The binding site of this exogenously added CO has been suggested to be

a potential site of reversible hydrogen oxidation. Binding of CO at the site results in an active site that is coordinately saturated with strong ligands (S, CO, and CN), thus providing a rational mechanism for inhibition of reversible hydrogen oxidation at the active site of CpI.

In this paper, we report the first infrared spectra for the oxidized and CO-inhibited forms of Fe-only hydrogenase I from *C. pasteurianum*. These spectra confirm that the oxidized form of the CpI hydrogenase contains a total of five diatomic ligands coordinated to the Fe ions of the active site [2Fe] subcluster. These spectra are in good agreement with the notion that these ligands are two terminally coordinated CO ligands, two terminally coordinated CN^- ligands, and a bridging CO ligand. On the basis of the pattern of bands detected in the IR spectra, a preliminary assignment of the relative placements of the ligands is presented. Finally, infrared spectra of the photoinduced intermediates as a function of irradiation temperature are reported. These spectra support the notion that there are at least two photoinduced events upon irradiation of the CO-inhibited form of the CpI hydrogenase and that the relative amounts of the two photoproducts are dependent on the temperature at which the irradiation is conducted. While the identity of this second intermediate remains somewhat uncertain, the infrared spectra place additional restrictions on its identity.

MATERIALS AND METHODS

Hydrogenase I from *C. pasteurianum* (CpI) was purified as described previously (*19*). The protein was equilibrated with 50 mM phosphate buffer (pH 7.0) containing 200 mM KCl and 2 mM sodium dithionite. The sample was then concentrated to approximately 3 mM. All manipulations were carried out in serum vials sealed with butyl stoppers and aluminum seals which had been degassed on a vacuum manifold with subsequent addition of Ar.

The enzyme was poised in the oxidized state by addition of excess thionin (>95%, Sigma) as previously described (*20*). The CO-inhibited state was generated by incubating the thionin-oxidized enzyme in the presence of either natural abundance CO or ^{13}CO (>99% ^{13}CO, <1% ^{18}O) for 5 min. ^{13}CO was acquired from Cambridge Isotope Laboratories (Andover, MA), and natural abundance CO was acquired from Matheson Gas Products (Cucamonga, CA).

Treated CpI was loaded into an anaerobic infrared transmittance cell using gastight Hamilton syringes inside an anaerobic chamber. The infrared cell had a path length of approximately 50 μm, and the window material was CaF_2. Low-temperature (6–300 K) infrared spectra were collected in a Bio-Rad FTS-40 FTIR spectrometer equipped with a low-temperature optical cryostat (ADP Cryogenics Heli-Tran LT-3-110, equipped with NaCl windows). The temperature of the sample was controlled via a Lakeshore Cryogenics temperature controller (DRC-80C). The sample cell was aligned at 45° to both the infrared beam and photolysis beam. Photolysis was achieved using white light from a 300 W xenon arc lamp (Oriel, 68811 arc lamp power supply) passed through a heat-absorbing filter. Light-induced difference spectra were determined by subtraction of the IR spectra collected in the dark from the IR spectra taken following irradiation for 10 min. To allow for the decay of light-induced species, the sample was warmed to 200 K in the dark
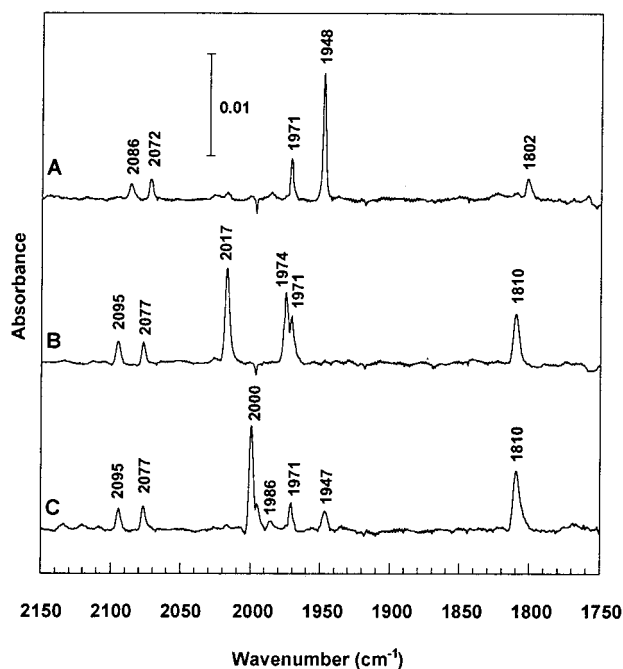
FIGURE 2: Absolute spectra of CpI hydrogenase at 20 K: (A) oxidized state, (B) CO-added oxidized state, and (C) ^{13}CO-added oxidized state.

following collection of each difference spectrum. The infrared spectra represent an average of 512 scans with a spectral resolution of 1 cm^{-1}.

RESULTS

The infrared spectra of CpI oxidized using thionin have infrared bands at 2086, 2072, 1971, 1948, and 1802 cm^{-1} as shown in Figure 2A. Upon incubation of the oxidized CpI with carbon monoxide (^{12}C and ^{16}O at natural abundance levels), the infrared bands of the oxidized enzyme are replaced with bands at 2095, 2077, 2017, 1974, 1971, and 1810 cm^{-1} as shown in Figure 2B. When the oxidized enzyme is instead incubated with ^{13}CO (>99% ^{13}C, <1% ^{18}O) the infrared bands at 2017, 1974, and 1971 cm^{-1} are replaced with three bands at 2000, 1947, and 1971 cm^{-1}, while the bands at 2095, 2077, and 1810 cm^{-1} are unaffected as shown in Figure 2C. A summary of the frequencies of the IR bands for the oxidized form of CpI, the ^{12}CO-added form of CpI, and the ^{13}CO-added form of CpI is shown in Figure 3.

Irradiation of the CO-added form of CpI (made using either ^{12}CO or ^{13}CO) at cryogenic temperatures (6−180 K) leads to significant changes in the infrared spectra. The differences associated with irradiation at the various temperatures are most apparent when difference spectra are determined between the infrared spectra recorded after irradiation and the spectra recorded in the dark just prior to irradiation. In the resultant light-minus-dark difference spectra, upward-moving bands arise from IR bands that appear (or increase in intensity) after irradiation, while downward-moving bands arise from infrared bands that disappear (or drop in intensity) upon irradiation. Light-minus-dark infrared difference spectra for ^{12}CO-added CpI recorded at various temperatures are shown in Figure 4, while light-minus-dark infrared difference spectra for ^{13}CO-added CpI recorded at various temperatures are shown in Figure 5. In both ^{12}CO-added CpI and ^{13}CO-
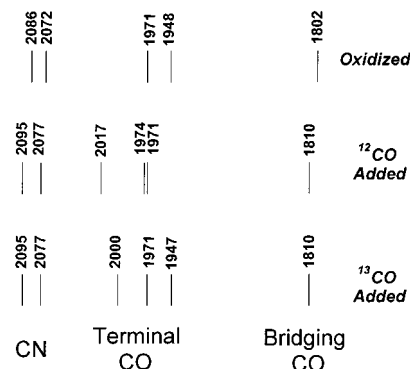

FIGURE 3: Summary of IR bands detected in the oxidized, ^{12}CO-added, and ^{13}CO-added states of the Fe-only hydrogenase from *C. pasteurianum.*
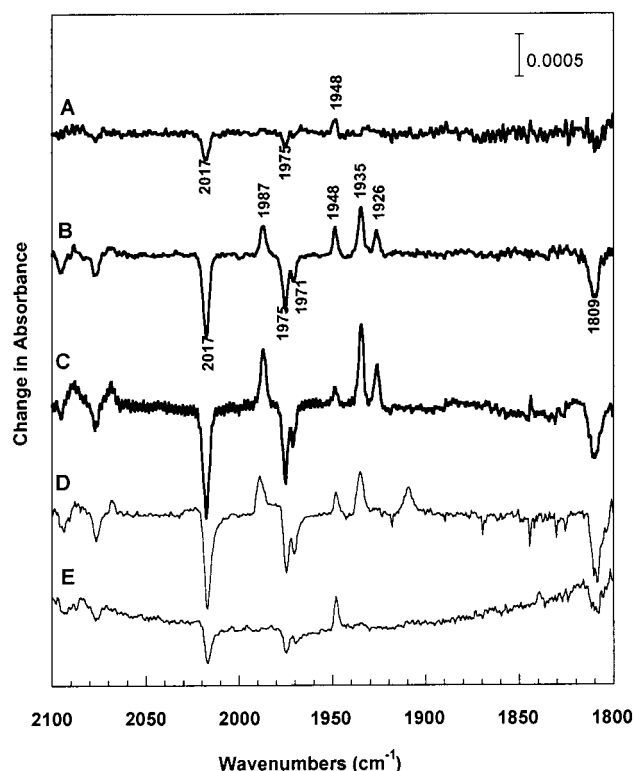

FIGURE 4: Light-minus-dark difference spectra for the CO-inhibited state CpI hydrogenase formed using natural abundance CO at (A) 6, (B) 30, (C) 40, (D) 80, and (E) 120 K. Difference spectra formed between the spectrum recorded in the dark and the spectrum recorded after irradiation for 10 min (irradiation for 20 min at 6 K) using white light passed through a heat-absorbing filter.

added CpI, the light-induced changes detected in the infrared spectra are reversed by warming the sample to 200 K in the dark.

In the light-minus-dark spectra, it is clear that the temperature at which the irradiation is conducted dramatically affects the pattern of bands detected in the IR spectrum between 2020 and 1800 cm^{-1}. The light-minus-dark infrared difference spectra recorded upon irradiation of the ^{12}CO-added state at 6 K (Figure 4A) show as their major contribution downward-moving bands at 2017 and 1975 cm^{-1} and a single upward-moving band at 1948 cm^{-1}. Irradiation of the ^{12}CO-added state at 30 K (Figure 4B) gives rise a different pattern of bands in the light-minus-dark difference spectrum, having downward-moving bands at 2017, 1975, 1971, and 1809 cm^{-1} and upward-moving bands at 1987,
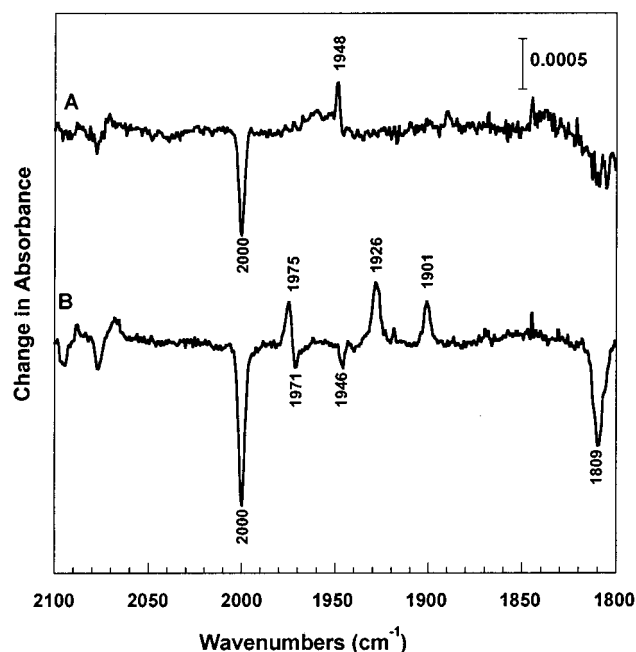
FIGURE 5: Light-minus-dark difference spectra for the CO-inhibited state formed using ^{13}CO at (A) 14 and (B) 40 K. (^{13}CO spectra at 40 K were corrected for contributions arising from ^{12}CO by performing a weighted subtraction as discussed in the text.) Difference spectra formed between the spectrum recorded in the dark and the spectrum recorded after irradiation for 10 min using white light passed through a heat-absorbing filter.

1948, 1935, and 1926 cm^{-1}. The pattern of bands detected in the 30 K difference spectra persists in the light-minus-dark difference spectra recorded between 30 and 80 K (Figure 4C,D), albeit with significant changes in the relative intensity of the 1948 cm^{-1} band compared to the other upward-moving bands. Additionally, the 1926 cm^{-1} band shifts to 1910 cm^{-1} for irradiation at the higher temperatures in this range. Finally, irradiation at 120 (Figure 4E), 140, and 160 K gives rise to difference spectra that once again resemble the light-minus-dark spectra recorded at 6 K with the sole upward-moving band detected at 1948 cm^{-1}, while irradiation at ≥180 K shows no bands in the light-minus-dark difference spectra.

A similar temperature dependence is seen in the light-minus-dark difference spectra recorded upon irradiation of the ^{13}CO-added state. Irradiation of the ^{13}CO state at 14 K has as its primary contribution a downward-moving band at 2000 cm^{-1} and an upward-moving band at 1948 cm^{-1} (Figure 5A), while irradiation at 40 K has downward-moving bands at 2000, 1971, 1946, and 1809 cm^{-1} and upward-moving bands at 1975, 1926, and 1901 cm^{-1}. The relative intensity of the 1948 cm^{-1} band compared to those of the other upward-moving bands is sensitive to the temperature at which the irradiation is carried out in a manner similar to what was seen in the ^{12}CO-added enzyme. In addition, no bands are detected in the difference spectra collected for irradiations carried out above 180 K. Finally, it should be noted that repeated irradiation of the ^{13}CO-added sample followed by warming to 200 K in the dark led to a systematic rise in contributions in the difference spectra that were identical to the difference spectra reported for the ^{12}CO-treated species. In fact, at all temperatures, it was possible to subtract that contribution from ^{12}CO difference spectra cleanly from the overall difference spectra.

DISCUSSION

The IR spectra of oxidized CpI hydrogenase have five bands in the 2100−1800 cm^{-1} spectral region, at 2086, 2072, 1971, 1948, and 1802 cm^{-1} (Figures 2A and 3). The pattern of bands is very similar to that in the IR spectra reported for the Fe-only hydrogenase from both *D. vulgaris* (*11*) and *D. desulfuricans* (*12*), showing a pair of high-intensity bands in the 1900−2000 cm^{-1} spectral region, a pair of infrared bands of somewhat lower intensity between 2100 and 2050 cm^{-1}, and a single band at frequencies between 1790 and 1820 cm^{-1}. In the IR spectrum of oxidized CpI, the two highest-intensity bands are detected at 1971 and 1948 cm^{-1}. These bands can be attributed to two terminal CO ligands coordinated to the Fe ions of the [2Fe] subcluster; their frequencies are in good agreement with stretching frequencies for terminally coordinated Fe carbonyls (*21*). Of particular significance is the fact that the frequencies that are detected are very similar to the frequency detected for the terminally coordinated CO ligand on the Fe ion in the [NiFe] hydrogenases. The stretching frequencies for the intrinsic CO in the [NiFe] hydrogenases fall between 1900 and 1980 cm^{-1} (depending on the redox state of the active site metals and the source of the NiFe hydrogenase that is being studied) (*6, 8, 12*). At higher frequencies are bands at 2086 and 2072 cm^{-1}. These bands fall in a frequency region consistent with their assignment as arising from two CN^{-} ligands coordinated to Fe. For comparison, we note that the two CN ligands coordinated to the active site Fe in the NiFe hydrogenases have frequencies between 2120 and 2060 cm^{-1}. A fifth infrared band is detected at 1802 cm^{-1}. This band can be assigned as a bridging CO ligand on the basis of its low frequency. Bridging CO ligands typically bond to both metal ions via coordination through the carbon and display infrared frequencies between 1850 and 1780 cm^{-1}, a frequency that is significantly lower than the stretching frequencies associated with terminally coordinated carbon monoxide ligands. In contrast, CN^{-} ligands typically bridge metal ions by coordination through both the carbon and nitrogen and display infrared stretching frequencies that are higher than those of their terminally coordinated counterparts (i.e., above 2100 cm^{-1}) (*21*).

X-ray crystallographic structures show that a single CO ligand binds to the outermost Fe (Fe2) of the [2Fe] subcluster when the oxidized enzyme is exposed to carbon monoxide (*17*). The infrared spectrum of this state has a total of six IR bands (Figures 2B and 3). Three bands (at 2017, 1974, and 1971 cm^{-1}) are found in the region associated with terminal CO ligands, consistent with the observation that a single exogenously added CO molecule binds to the outermost Fe of the active site's [2Fe] subcluster. Upon exposure of the oxidized enzyme to CO, the bridging CO shifts to 1810 cm^{-1}. Detection of a band at 1810 cm^{-1} upon binding of exogenously added CO at Fe2 confirms that the bridging CO found in the oxidized state retains its bridging character after binding of the exogenously added CO at Fe2.

Relative Placement of Terminally Coordinated CO or CN^{-} Ligands in the [2Fe] Subcluster. As previously discussed, the IR spectra and X-ray crystallographic structure for the oxidized Fe-only hydrogenase are consistent with the notion that nonprotein ligands L1−L4 can be identified as two terminally coordinated CO and two terminally coordinated

CN ligands in the H-cluster of the Fe-only hydrogenases. On the basis of the fact that amino acid residues are found near L2 and L4 which can act as H-bond donors, it has been proposed that L2 and L4 may be the CN ligands. L1 and L3 which are found in a hydrophobic pocket have been proposed to be the two CO ligands (*10*). This gives rise to a [2Fe] subcluster with a mixed ligand system (one CO and one CN) on each of the two Fe ions. However, on the basis of the pattern of infrared bands detected in the oxidized enzyme alone, either a mixed ligand system with placement of one CO on each Fe of the [2Fe] cluster or placement of both CO ligands on one Fe and both CN^- ligands on the other is consistent with the IR spectrum for the oxidized state. To distinguish between these models, examination of the pattern of bands resulting from exposure of the enzyme to exogenously added CO, which X-ray studies confirm binds at Fe2, is instructive. This examination supports the placement of one of the two intrinsic CO ligands on each of the Fe atoms of the [2Fe] subcluster. The arguments are as follows. (1) The fact that the infrared spectra exhibit a total of three bands that can be attributed to CO ligands argues against placing all three CO ligands on the same metal center (two intrinsic CO ligands and one exogenous CO ligand, all on Fe2) since in the absence of significantly different coupling constants between the three CO ligands, only two IR bands would be predicted for this scenario (two of the three possible modes in this case being degenerate) (*22*). (2) The band at 1971 cm^{-1} can be attributed to an intrinsic CO since it appears in both the oxidized and CO-added spectra. Furthermore, the fact that it does not shift in frequency upon addition of exogenous CO argues against placing it on the same Fe as the exogenous CO (i.e., placement on Fe2); addition of CO to a metal center gives rise to a decrease in charge density which will be reflected as a significant increase in the CO stretching frequency for any other CO ligands on the same metal center. In contrast, the 1948 cm^{-1} band in the oxidized spectrum can be attributed to an intrinsic CO coordinated to the same Fe as the exogenous CO. Upon addition of CO, the 1948 cm^{-1} band disappears and a pair of bands at 2017 and 1974 cm^{-1} appear. This can be understood as follows. Addition of exogenous CO to Fe2 gives rise to two coupled CO vibrations arising from vibrational coupling between the two resultant CO ligands on Fe2. Their frequencies are higher than before addition of the exogenous CO because addition of CO (a good π-acceptor) decreases the charge density at Fe2. (3) The pattern of bands detected when the enzyme is incubated with ^{13}CO rather than natural abundance CO is also consistent with the placement of one of the intrinsic ligands on Fe2 and the other on Fe1 (Figure 2C). In ^{13}CO, the exogenous CO is ^{13}CO but the intrinsic CO ligands are still ^{12}CO. In that case, one expects that both of the bands arising from the CO ligands on Fe2 in the CO-added enzyme (one intrinsic and one exogenous CO) will shift in ^{13}CO. However, the intrinsic CO ligated to Fe1 should be unaffected. This is in agreement with what is observed. The 2017 and 1974 cm^{-1} bands detected in natural abundance CO shift to 2000 and 1947 cm^{-1} in ^{13}CO, but the 1971 cm^{-1} band is unaffected. Taken together, these arguments provide compelling evidence that one of the two intrinsic ligands is not coordinated to the same Fe as the exogenously added CO (i.e., is not on Fe2 and must be on Fe1) while the other intrinsic CO ligand is

Table 1: Comparison of the Infrared Bands That Can Be Attributed to the Active Site Carbon Monoxide and Cyanide Ligands in the Fe-Only Hydrogenases from *C. pasteurianum* and *D. desulfuricans*

state	assignment	IR frequency (cm^{-1})	
		C. pasteurianum I	*D. sulfuricans*[a]
oxidized	CN_1	2086	2093
	CN_2	2072	2079
	CO_{Fe1}	1971	1965
	CO_{Fe2}	1948	1940
	CO_{bridge}	1802	1802
^{12}CO-added	CN_1	2096	2096
	CN_2	2077	2087
	CO_{Fe1}	1971	1963
	$CO_{Fe2(sym)}$	2017	2016
	$CO_{Fe2(asym)}$	1974	1972
	CO_{bridge}	1810	1811

[a] Data from ref *12*.

coordinated to the same Fe as the exogenously added CO (i.e., is on Fe2).

Comparison of the Infrared Spectra for the Fe-Only Hydrogenases from C. pasteurianum (I) and D. desulfuricans. The behavior of the infrared bands arising from the CO ligands upon incubation in carbon monoxide is quite similar for the Fe-only hydrogenase I from *C. pasteurianum* (reported herein) and that reported for the Fe-only hydrogenase from *D. desulfuricans* reported by Fernandez and co-workers (*12*). The frequencies of the IR bands arising from the CO and CN ligands in the two enzymes are summarized in Table 1. In both enzymes, one of the CO bands detected in the infrared spectrum of the oxidized enzyme can be attributed to an intrinsic CO ligand on Fe1, as it shifts very little when exogenous CO binds, and the other CO band detected in the oxidized enzyme can be assigned to an intrinsic CO on Fe2 because it shifts upward in frequency and becomes vibrationally coupled to the exogenous CO when ^{12}CO binds at Fe2. Additionally, in both cases, the bridging CO vibration shifts upward by almost the same amount upon exogenous CO binding at Fe2. In addition, for both enzymes, *both* CN vibrations shift upward upon CO binding at Fe2. It not clear why this should be so. In both enzymes, the IR band that can be attributed to the intrinsic CO coordinated to Fe1 is largely unaffected by CO binding at Fe2, suggesting that CN binding at Fe2 does not significantly alter the charge density at Fe1. One possibility is that the vibrations arising from the CN ligands might be vibrationally coupled despite the fact they are on separate Fe ions. The upward shift in both CN bands might then arise from both a change in the charge density at Fe2 upon CO binding and a concomitant change in the degree of vibrational coupling between the CN vibrations when the exogenous CO binds at Fe2. Further experiments are planned to assess this possibility. Finally, it should be noted that the degree by which the two CN vibrations shift upon exogenous CO binding to Fe2 is quite different in the two enzymes. While this is not understood at present, it is interesting to note that the amino acids that have been identified as putative hydrogen bond donors for the CN ligand on Fe1 are quite different. In the case of CpI, the side chain of Ser[252] has been proposed to act as a hydrogen bond donor to the CN ligand on Fe1, while in *D. desulfuricans*, the amide of the peptide backbone plays this role (*9, 10*).

Light-Induced Species Formed upon Irradiation at Cryogenic Temperatures. Irradiation of the CO-inhibited enzyme at cryogenic temperatures gives rise to changes in the IR spectra that are dependent on the temperature at which the photolysis is carried out. Upon irradiation of the ^{12}CO-added enzyme at 6 K, bands attributed to the three terminally coordinated CO ligands (at 2017, 1974, and 1971 cm^{-1}) disappear and are replaced by a single band at 1948 cm^{-1} (Figure 4A). This pattern is consistent with what is expected upon photolysis of the exogenous CO from Fe2. Photolysis of the exogenous CO should give rise to an IR spectrum that is quite similar to the oxidized spectrum, and the light-minus-dark difference spectrum arising from photolysis of the exogenous CO would be expected to have downward-moving bands at 2017 and 1974 cm^{-1} and an upward-moving band at 1948 cm^{-1}. (The 1971 cm^{-1} band that is present in the IR spectra of both the CO-inhibited and oxidized states and will be detected in the difference spectra only to the extent that its extinction coefficient differs between the oxidized and CO-inhibited forms.)

The light-induced difference spectrum formed upon irradiation at 14 K for the CO-added state prepared with ^{13}CO is also consistent with this explanation (Figure 5A). In this case, a single upward-moving band is detected at 1948 cm^{-1}, a frequency identical to that detected upon irradiation of the ^{12}CO-exposed sample. Hence, upon irradiation at 6−14 K, the CO-inhibited state is converted into a state in which the $\nu(CO)$ bands are no longer sensitive to ^{13}CO labeling of the exogenous CO. This is what would be expected if irradiation at 6−14 K only photolyzes the exogenously added CO (in this case, the ^{13}CO) from Fe2.

Irradiation at 30 K gives rise to a very different IR difference spectrum when compared to the spectrum for irradiation at 6−14 K. In the case of the CO-inhibited state prepared using ^{12}CO (i.e., natural abundance CO), the magnitude of the 1810 cm^{-1} band decreases and the bands attributed to CO at 2017, 1974, and 1971 cm^{-1} are replaced with bands at 1987, 1948, 1935, and 1926 cm^{-1} (Figure 4B). The $\nu(CN)$ bands also shift upon irradiation from 2095 to 2089 cm^{-1} and from 2077 to 2068 cm^{-1}. This pattern of light-induced bands persists when irradiation is carried out at temperatures between 20 and 80 K, albeit with some differences in the relative intensities for the 1948 cm^{-1} band as compared to the 1987, 1935, and 1926 cm^{-1} bands (Figure 4). Additionally, starting with irradiation at 60 K, the light-induced 1926 cm^{-1} band appears to be replaced with a band at 1910 cm^{-1}. For irradiation at temperatures above 80 K, the light-induced 1948 cm^{-1} band gains in intensity significantly compared to the 1987, 1935, and 1926/1910 cm^{-1} bands, and starting at 120 K, it becomes the predominant feature. Finally, for temperatures above 180 K, no changes are detected in the IR spectra upon irradiation.

If the CO-inhibited form of the enzyme is made using ^{13}CO, irradiation at temperatures above 30 K also gives rise to a different pattern of bands in the difference spectra as compared to the spectra for irradiation at 14 K (Figure 4B). Once again, the 1810 cm^{-1} band is lost and the CN bands shift from 2095 to 2089 cm^{-1} and from 2077 to 2068 cm^{-1}. However, bands that can be attributed to the terminal CO ligands after irradiation of the ^{13}CO-inhibited enzyme are quite different from what is seen in the ^{12}CO-inhibited enzyme. Upon irradiation at 20−60 K, bands at 2000, 1971,

and 1946 cm^{-1} are replaced with bands at 1975, 1926, and 1901 cm^{-1}. Hence, after irradiation, the species formed is still sensitive to isotopic labeling of the exogenous CO (the light-induced bands at 1987 and 1935 cm^{-1} in the ^{12}CO-inhibited enzyme are replaced by light-induced bands at 1975 and 1901 cm^{-1}, respectively, in the ^{13}CO-inhibited enzyme), suggesting that the ^{13}CO remains coordinated at the active site (most probably at Fe2) following irradiation at temperatures above 20 K. In contrast, the light-induced 1926 cm^{-1} band is unaffected by ^{13}CO exposure and therefore may arise from the intrinsic CO on Fe1.

Comparing the 6−14 K light-minus-dark difference spectra to the difference spectra collected above 30 K, we can conclude that irradiation gives rise to at least two different light-induced species, the relative amount of which is dependent on the temperature at which the irradiation is carried out. One of the species is characterized by the presence of a CO band at 1948 cm^{-1}. This species is detected at all irradiation temperatures below 160 K. It is the sole species detected upon irradiation at 6−14 K and becomes the predominant species detected for irradiation between 100 and 160 K. As discussed previously, the pattern of IR bands detected in the IR spectra for this species is consistent with the notion that irradiation at 6−14 K gives rise to the photolytic loss of the exogenously added CO from Fe2 as shown in Figure 6A. This is in agreement with conclusions drawn from the EPR studies of Adams and co-workers where irradiation at 8 K gave rise to the conversion of the axial 2.07 signal to a rhombic 2.10 signal (*16*). In both the EPR and IR studies, the signals arising from this photoinduced state decay above 150 K, suggesting that above 150 K rebinding of the exogenously added CO to Fe2 occurs. Recent X-ray crystallographic studies also support this assignment; the F_o(illuminated) − F_o(nonilluminated) electron density map for the CO-inhibited state indicates that the exogenous CO is photolytically cleaved from Fe2 upon irradiation with a helium−neon laser at 80−100 K (*18*).

The second light-induced species gives rise to significantly different IR spectra with $\nu(CO)$ bands at 1987, 1935, and 1926 cm^{-1}. In addition, the 1809 cm^{-1} band arising from the bridging CO is lost upon its formation. This species is not detected upon photolysis at 6−14 K but becomes the predominant feature for irradiation temperatures between 30 and 60 K. For irradiation at temperatures above 80 K, this species is no longer detected, suggesting that this photoinduced species reverts to the ground state (i.e., the CO-inhibited form present in the dark) above 80 K. This behavior is consistent with the recombination of the photolysis product to the active site for temperatures above 80 K and is very similar to the behavior of the light-induced rhombic 2.26 signal described by Adams and co-workers. The decay of this species above 80 K also provides a rationale for why a second light-induced species was not detected in recent X-ray crystallographic studies on the CO-inhibited state of CpI upon irradiation at cryogenic temperatures, since those studies were carried out at temperatures slightly above the decay temperature for the second light-induced species (80−100 K) and used a weak helium−neon laser as the light source (*18*).

The loss of the IR band at 1809 cm^{-1} in the second light-induced species provides strong evidence that the bridging CO ligand of the dark-induced species loses its bridging character upon irradiation. This may be the result of either

(A)

$\nu CO_{bridge} = 1809$
$\nu CO_{Fe1} = 1971$
$\nu CO_{Fe2} = 2017/1974$ (coupled)
$[\nu CO_{Fe2} = 2000/1947$ in ^{13}CO added]

(B)

$\nu CO_{bridge} = 1809$
$\nu CO_{Fe1} = 1971$
$\nu CO_{Fe2} = 2017/1974$ (coupled)
$[\nu CO_{Fe2} = 2000/1947$ in ^{13}CO added]

$\nu CO_{bridge} = 1802$
$\nu CO_{Fe1} = 1971$
$\nu CO_{Fe2} = 1948$

I

OR

II

$\nu(CO)_{bridge}$ is lost
$\nu CO_{Fe1} = 1926$
$\nu CO_{Fe2} = 1987/1935$ (coupled)
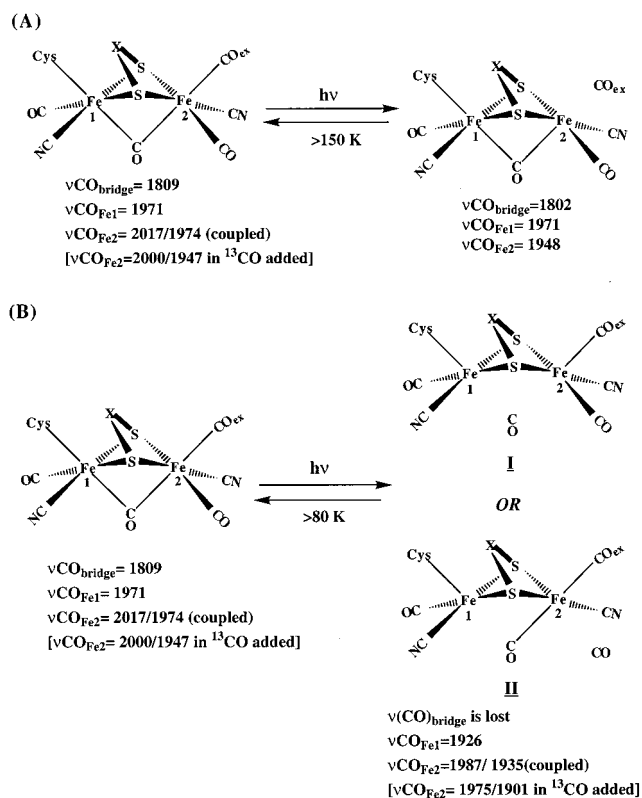$[\nu CO_{Fe2} = 1975/1901$ in ^{13}CO added]

FIGURE 6: Models depicting the two light-induced states detected using infrared spectroscopy. (A) The first light-induced species arises from the photolytic loss of the exogenous CO and decays above 150 K. (B) The second light-induced species is characterized by the loss of the bridging character in the Fe bridging CO. This species decays above 80 K. Two models are consistent with this species: the photolytic loss of the bridging CO from both Fe1 and Fe2, depicted as **I**, and the photolytic loss of the intrinsic CO on Fe2 accompanied by the conversion of the bridging CO into a terminally coordinated CO on Fe2, depicted as **II**. Proposed band assignments for infrared bands detected in the light-minus-dark infrared difference spectra are summarized.

the bridging CO being converted to a terminal CO ligand upon irradiation or complete photolysis of the bridging CO from the Fe ions. With regard to these possibilities, it should be noted that both scenarios have been shown to occur upon irradiation of the binuclear Fe complex, $Fe_2(CO)_9$, which contains three bridging CO ligands and an Fe—Fe bond. Poliakoff and Turner (*23*) have shown that irradiation of $Fe_2(CO)_9$ gives rise to the loss of one of the bridging carbonyls, generating $Fe_2(CO)_8$ in two different isomeric forms. The first form contains two bridging carbonyls and has three terminally coordinated carbonyls on each of the two Fe ions, while the second form has four terminally coordinated carbonyls on each Fe ion. Additionally, we note that crystallographic structures of the reduced state in *D. desulfuricans* suggest that the bridging CO may adopt a terminal configuration on Fe2 upon reduction (*24*).

When these two models are being considered, it should be noted that the pattern of IR bands associated with this second light-induced species places some constraints on the nature of this species. First, as the 1809 cm^{-1} band is lost, the $\nu(CO)$ stretches for all CO ligands shift downward significantly (from 2017, 1974, and 1971 cm^{-1} to 1987, 1935, and 1926/1910 cm^{-1}, respectively). The $\nu(CN)$ stretches also shift downward slightly from 2095 to 2089 cm^{-1} and from 2077 to 2068 cm^{-1}. This suggests that as the bridging

character of this CO is lost, the charge density at both Fe sites increases. Second, following irradiation there are still at least three IR bands that can be attributed to terminally coordinated CO ligands (at 1986, 1936, and 1925/1910 cm^{-1}). Hence, following irradiation there must be at least three terminally coordinated CO ligands present in the active site. Finally, following irradiation of the ^{13}CO-inhibited enzyme, two of the bands that can be attributed to terminally coordinated CO are sensitive to whether the enzyme was exposed to ^{13}CO or ^{12}CO, and this suggests that the ^{13}CO that was present on Fe2 before irradiation remains on Fe2 after irradiation in this species. In addition, the fact that a second light-induced band also shifts in the ^{13}CO-inhibited enzyme suggests that the ^{13}CO remains vibrationally coupled to at least one other terminally coordinated CO ligand following irradiation.

Considering potential models for the nature of the second light-induced species, namely, one in which the photoinduced species arises from complete loss of the bridging ligand or one that includes the possibility that the irradiation converts the bridging ligand into a terminally coordinated CO, we note that all three conditions are readily met if the bridging ligand is completely photolyzed from both Fe ions upon irradiation (**I** in Figure 6B). A bridging CO is a good π-acceptor. The removal of the bridging CO from both Fe atoms is therefore expected to give rise to a downward shift in the frequencies associated with the CO and CN ligands coordinated to both Fe1 and Fe2, as is detected. In this case, the presence of effects arising from ^{13}CO after irradiation would remain provided that in this photoinduced state the exogenously added CO remains on Fe2 (**I** in Figure 6B).

The photolytic conversion of the bridging CO into a terminally coordinated CO cannot be excluded since such an event would also lead to the loss of the 1809 cm^{-1} band (**II** in Figure 6B). However, the IR data place a number of restrictions on the nature of the photoinduced species for this case. (1) The conversion from a bridging CO to a terminally coordinated CO must occur such that the bond between the bridging CO and Fe1 is broken so as to account for the downward shift in frequency on the $\nu(CO)$ band assigned to the CO on Fe1 (1971 cm^{-1} shifts to 1926 cm^{-1}). This implies that the bridging CO must become terminally coordinated to Fe2 rather than to Fe1 upon irradiation. (2) The photoconversion of the bridging CO into a terminally coordinated CO on Fe2 must be accompanied by a significant increase in charge density at Fe2 since the $\nu(CO)$ stretches associated with Fe2 carbonyls all shift down significantly in frequency (2017 and 1974 cm^{-1} shift to 1986 and 1935 cm^{-1}, respectively) upon irradiation. This would appear to require that as the bridging carbonyl becomes a terminally coordinated CO on Fe2, one of the other terminally coordinated CO ligands on Fe2 must be lost. (If both of the other terminally coordinated CO were to remain after irradiation, a total of three terminally coordinated CO ligands would then be present on Fe2, leading to an upward shift in frequency for these bands.) (3) The exogenously bound CO must remain on Fe2 after the photoconversion. The infrared difference spectra of the CO-inhibited state made using ^{13}CO show that two of the three bands in the light-induced spectra are affected by ^{13}CO (1987 and 1935 cm^{-1} in ^{12}CO and 1975 and 1901 cm^{-1} in ^{13}CO). This suggests that the exogenously bound CO is not photolyzed from Fe2 in this state. It also

suggests that it remains vibrationally coupled to the ν(CO) arising from at least one other terminally coordinated CO on Fe2. To satisfy this criterion, it appears that the intrinsic CO ligand on Fe2 (L3) would need to be lost upon irradiation and the subsequent conversion of the bridging CO to a terminally coordinated CO on Fe2, as shown in **II** of Figure 6B. We note that to detect both the symmetric and asymmetric combinations for the two CO ligands in this model we must also assume that the protein environment breaks the symmetry between the two remaining CO ligands on Fe2, despite the fact that they are expected to be roughly trans to each other following the photoconversion.

CONCLUSIONS

The infrared spectra of CpI support the notion that the active site contains two terminally coordinated CO ligands, two terminally coordinated CN$^-$ ligands, and a bridging CO. The pattern of bands detected in the IR spectra is in agreement with the placement of the terminally coordinated CO and CN$^-$ ligands such that each of the two Fes of the [2Fe] subcluster is ligated to one CO and one CN ligand.

Infrared spectra of species formed upon irradiation at cryogenic temperatures show that at least two species are formed upon irradiation, the relative proportions of which are dependent on the temperature at which the irradiation is carried out. Irradiation at 6−14 K gives rise to an infrared spectrum that is consistent with the photolytic loss of the exogenous CO from Fe2. Above 150 K, this component decays in a manner consistent with rebinding of the exogenous CO to Fe2. Irradiation at temperatures above 20 K gives rise to an additional species characterized by the loss of bridging character for the bridging CO. This light-induced species decays above 80 K and appears to be correlated with the detection of the rhombic 2.26 signal previously reported by Adams and co-workers (*16*). While the nature of this additional light-induced species remains somewhat unclear on the basis of the IR results reported herein, the IR spectra do place additional constraints on the nature of this species. Two models that are consistent with these observations are depicted in Figure 6B. In the first model (**I** in Figure 6B), the loss of the 1809 cm^{-1} band and concurrent downward shift of the ν(CN) and ν(CO) stretches associated with the terminally coordinated ligands are explained by the photolytic loss of the bridging CO from both Fe ions of the [2Fe] subcluster. In the second model (**II** in Figure 6B), the loss of the 1809 cm^{-1} band is explained by assuming that the bridging CO is photolytically converted into a terminally coordinated CO on Fe2. In this model, the downward shift of the ν(CO) and ν(CN) frequencies is explained by the concurrent photolytic loss of another terminally coordinated CO from Fe2. The sensitivity of the light-induced bands to ^{13}CO is explained by assuming that in this species the terminally coordinated CO that is lost from Fe2 is the intrinsic CO ligand rather than the exogenous CO ligand.

In closing, we note that infrared studies provide insight into small cluster rearrangements that accompany oxidation state changes and CO inhibition, at a level which is on the order of coordinate error in the X-ray crystallographic studies.

In addition, the photolability studies reported herein provide a sensitive measure of the relative stability versus lability of the CO and CN ligands in the active site of the Fe-only hydrogenases. These studies support the notion that the cluster arrangement provides an assembly of more or less stably bound diatomic species which tune the chemistry of the cluster while at the same time providing labile sites that allow for the maintenance of ligand exchangeable sites for hydrogen oxidation chemistry.

REFERENCES

1. Volbeda, A., Charon, C. H., Piras, C., Hatchikian, E. C., Frey, M., Frey, M., and Fontecilla-Camps, J. C. (1995) *Nature 373*, 580−587.
2. Higuchi, Y., Yagi, T., and Yasouka, N. (1997) *Structure 5*, 1671−1680.
3. Pierik, A. J., Roseboom, W., Happe, R. P., Bagley, K. A., and Albracht, S. P. J. (1999) *J. Biol. Chem. 274*, 3331−3337.
4. Happe, R. P., Roseboom, W., and Albracht, S. P. J. (1999) *Eur. J. Biochem. 259*, 602−608.
5. Bagley, K. A., Van Garderen, C. J., Chen, M., Duin, E. C., Albracht, S. P. J., and Woodruff, W. H. (1994) *Biochemistry 33*, 9929−9236.
6. Bagley, K. A., Duin, E. C., Roseboom, W., Albracht, S. P. J., and Woodruff, W. H. (1995) *Biochemistry 34*, 5527−5535.
7. Van Der Spek, T. M., Bagley, K. A., Arendsen, A. F., Happe, R. P., Yun, S., Bagley, K. A., Stufkens, D. J., Hagen, W. R., and Albracht, S. P. J. (1996) *Eur. J. Biochem. 237*, 629−634.
8. Happe, R. P., Roseboom, W., Pierik, A. J., Albracht, S. P. J., and Bagley, K. A. (1997) *Nature 385*, 126.
9. Peters, J. W., Lanzilotta, W. N., Lemon, B. J., and Seefeldt, L. C. (1998) *Science 282*, 1853−1858.
10. Nicolet, Y., Piras, C., Legrand, P., Hatchikian, C. E., and Fontecilla-Camps, J. C. (1999) *Structure 7*, 13−23.
11. Pierik, A. J., Hulstein, M., Hagen, W. R., and Albracht, S. P. J. (1998) *Eur. J. Biochem. 258*, 572−578.
12. De Lacey, A. L., Stadler, C., Cavazza, C., Hatchikian, E. C., and Fernandez, V. M. (2000) *J. Am. Chem. Soc. 122*, 11232−11233.
13. Adams, M. W. W. (1990) *Biochim. Biophys. Acta 1020*, 115−145.
14. Erbes, D. L., Burris, R. H., and Orme-Johnson, W. H. (1975) *Proc. Natl. Acad. Sci. U.S.A. 72*, 4795.
15. Bennett, B., Lemon, B. J., and Peters, J. W. (2000) *Biochemistry 39*, 7455−7460.
16. Kowal, A. T., Adams, M. W. W., and Johnson, M. K. (1989) *J. Biol. Chem. 264*, 4342−4348.
17. Lemon, B. J., and Peters, J. W. (1999) *Biochemistry 38*, 12969−12973.
18. Lemon, B. J., and Peters, J. W. (2000) *J. Am. Chem. Soc. 122*, 3793−3794.
19. Chen, J. S., and Mortenson, L. E. (1974) *Biochim. Biophys. Acta 371*, 283−298.
20. Adams, W. W. (1987) *J. Biol. Chem. 262*, 15054−15061.
21. Nakamoto, K. (1997) *Infrared and Raman Spectra of Inorganic and Coordination Compunds, Part B: Applications in Coordination, Organometallic, and Bioinorganic Chemistry*, 5th ed., John Wiley and Sons, New York.
22. Braterman, P. S. (1975) *Metal Carbonyl Spectra*, Academic Press, New York.
23. Poliakoff, M., and Turner, J. J. (1971) *J. Chem. Soc. A*, 2403−2410.
24. Nicolet, Y., De Lacey, A. L., Vernede, X., Fernandez, V. M., Hatchikian, E. C., and Fontecilla-Camps, J. C. (2001) *J. Am. Chem. Soc. 123*, 1596−1601.